Elastic, piezoelectric, and dielectric properties of multidomain $0.67Pb(Mg_{1/3}Nb_{2/3})O_3-0.33PbTiO_3$ single crystals

Rui Zhang, Bei Jiang, and Wenwu Cao[a)]
Materials Research Laboratory, The Pennsylvania State University, University Park, Pennsylvania 16802

(Received 18 April 2001; accepted for publication 11 June 2001)

The elastic, piezoelectric, and dielectric constants of $0.67Pb(Mg_{1/3}Nb_{2/3})O_3-0.33PbTiO_3$ domain engineered single crystal were determined experimentally by using ultrasonic and resonance methods. It was confirmed that the single crystal system has large electromechanical coupling coefficient k_{33} (~94%) and piezoelectric constant d_{33} (~2800 pC/N) if the poling is done along the [001] of pseudocubic directions. A soft shear mode with a velocity of 880 m/s was observed in the [110] direction with displacement in $[\bar{1}10]$. Using the measured data, the orientation dependence of phase velocities and electromechanical coupling coefficients were calculated. The origin of experimental errors and their influence on measured results are also examined. © *2001 American Institute of Physics.* [DOI: 10.1063/1.1390494]

I. INTRODUCTION

Relaxor based ferroelectric single crystal systems, $Pb(Zn_{1/3}Nb_{2/3})O_3-PbTiO_3$ (PZN–PT) and $Pb(Mg_{1/3}Nb_{2/3})O_3-PbTiO_3$ (PMN–PT) exhibit extraordinary large electromechanical coupling coefficient k_{33} (>90%) and piezoelectric coefficient d_{33} (>2000 pC/N) at room temperature after being poled in [001] of the cubic coordinates.[1–5] Such high electromechanical coupling coefficient and piezoelectric coefficient values make the domain engineered single crystal systems very useful for producing higher sensitivity ultrasonic transducers with superior broadband characteristics, large strain actuators, and many other electromechanical devices.[6–7] For these systems, because the dipoles in each unit cell are formed along ⟨111⟩ of the cubic parent phase, the poling along [001] produces a multidomain structure, which is macroscopically pseudotetragonal.

The mechanism that causes the domain engineered single crystal systems to have such large electromechanical properties is still not well understood. The lack of complete physical property data is the main hindrance for further theoretical studies. It is also very important for device designers to have a complete set of elastic, piezoelectric, and dielectric constants since many simulation packages require the complete data set as input. Previously, we have published a complete set of elastic, piezoelectric, and dielectric constants for domain engineered single crystal PZN–4.5%PT.[8] However, it was found that the PMN–PT system can have a larger electromechanical coupling coefficient k_{33} and is mechanically more stable than the PZN–PT system. In addition, larger size PMN–PT single crystals are now readily available from many crystal growers. In this article we report one complete set of elastic, piezoelectric, and dielectric constants for the 0.67PMN–0.33PT domain engineered single crystal, which has the best properties among all the crystal compositions of this system.

[a)]Author to whom correspondence should be addressed; electronic mail: cao@math.psu.edu

The foremost concern to device designers is the reported high electromechanical properties. Our experimental results indeed confirmed that the 0.67PMN–0.33PT single crystal system has an electromechanical coupling coefficient k_{33} of 94% and piezoelectric constant d_{33} of 2800 pC/N. Similar to the PZN–4.5%PT system reported earlier, a soft shear mode with a velocity of 880 m/s was observed in the [110] direction with the displacement polarized in $[\bar{1}10]$.

Quite different from characterizing single domain single crystals, we found that the properties of these multidomain samples depend strongly on the domain patterns that are generated in the poling process, or the effective symmetry associated with the domain patterns of the system. This domain pattern dependence often creates inconsistencies when more than one sample is used for characterization, particularly when these samples have different geometry, such as those used in the resonance measurements. In this article, we will also analyze the origins of experimental errors and point out the error influence on particular measured constants.

II. EXPERIMENTAL PROCEDURE

The experimental setup and procedure are similar to that used in Ref. 8, except for some small modifications that were made in the averaging method to improve measurement accuracy. Several batches of samples have been used to ensure the self-consistency of the final results.

At room temperature, the 0.67PMN–0.33PT single crystals are in the ferroelectric phase with rhombohedral ($3m$) symmetry. From the phase diagram of PMN–PT, 0.67PMN–0.33PT is near the morphotropic boundary (~35% PT). It has been shown experimentally that the crystal can hold the highest level of stable macroscopic polarization only when the poling field is applied along one of the six ⟨100⟩ directions of the cubic axes.[6,7] Such a poling field direction will create a multidomain structure since there are still four remaining degenerate polarization orientations, [111], $[\bar{1}11]$, $[1\bar{1}1]$, and $[\bar{1}\bar{1}1]$, remaining in the crystal after poling. If the number of domains is large enough, statistically speaking, the global macroscopic symmetry can be treated as a

TABLE I. The relationships between phase velocities and elastic constants for $4mm$ symmetry and the measured values of phase velocities in PMN–33%PT multidomain single crystals poled in [001] of cubic axes.

Phase velocities	$v_l^{[001]}$	$v_s^{[001]}$	$v_l^{[100]}$	$v_{s\perp}^{[100]}$	$v_{s\parallel}^{[100]}$	$v_l^{[110]}$	$v_{s\perp}^{[110]}$	$v_{s\parallel}^{[110]}$
Related elastic constants	c_{33}^D	c_{44}^E	c_{11}^E	c_{66}^E	c_{44}^D	$\frac{1}{2}(c_{11}^E+c_{12}^E+2c_{66}^E)$	$\frac{1}{2}(c_{11}^E-c_{12}^E)$	c_{44}^D
Value of measured velocity (m/s)	4610	2930	3792	2882	3099	4727	880	3090

pseudotetragonal $4mm$ as discussed in Ref. 7. For the tetragonal symmetry, there are a total of 11 independent electro–elastic constants: six elastic, three piezoelectric, and two dielectric constants to be determined.

In principle, all independent elastic, piezoelectric, and dielectric constants for crystals with any symmetry can be determined either by the resonance method or by the ultrasonic method alone, so long as sufficient numbers of differently oriented samples are available.[9] In reality, however, for materials of lower symmetry, some geometries for resonance measurements are difficult to obtain, especially when the available crystal is too small to make large aspect ratio free resonators. On the other hand, since the ultrasonic technique can only directly measure certain constants through the measurements of pure mode phase velocities, large errors may be introduced for those material derived constants that are not related to pure modes.[10] High acoustic attenuation of certain modes may also damp the propagation of ultrasonic waves of certain modes so that a complete set of material constants for the low symmetry system is also difficult to obtain by using the ultrasonic method alone. Over the past few years, we have developed a hybrid method by combining the ultrasonic and resonant technique, so that the least number of samples are needed to resolve the problem of property variation from sample to sample and also to eliminate some of the unreliable geometries in the resonance method.[11]

The PMN–PT crystal samples were made in the Piezocrystal Resource at the Pennsylvania State University. The as grown crystals are orientated using the Laue method with an orientation accuracy of $\pm 0.5°$. Then, samples were cut into different geometries and dimensions based on the requirements of different types of measurements. The final dimensions of the samples used for the ultrasonic measurements were $4\times4\times2$ mm^3. For the length extensional and the thickness resonance measurements, the aspect ratio of the sample exceeded 5:1 in order to yield nearly pure resonance modes.[9] Gold electrodes were sputtered onto the parallel surface of samples for poling. An external electric field of 1.0–1.5 MV/m was applied at room temperature along the [001] direction of cubic axes to pole these samples into pseudotetragonal structure.

A 15 MHz longitudinal wave transducer (Ultran Laboratories, Inc.) and a 20 MHz shear wave transducer (Panametrics) were used for the pulse–echo measurements. The electric pulses used to excite the transducer were generated by a Panametrics 200 MHz pulser/receiver, and the time-of-flight between echoes was measured by a Tektronix 460 A digital oscilloscope. For a crystal with tetragonal $4mm$ symmetry, sound velocities can be directly measured for eight independent pure modes. From each measurement, either one elastic constant or a linear combination of several elastic constants can be obtained as shown in Table I. It is seen that c_{44}^D and c_{12}^E can be determined by more than one measurements, which provides a control check.

In resonant measurements, two length-extension resonators and one thickness resonator are used. A HP 4194 A impedance/gain-phase analyzer was employed to measure the resonance and antiresonance frequencies of these resonators. From the resonance and antiresonance frequencies, three electromechanical coupling coefficients k_{31}, k_{33}, k_t and three elastic compliance s_{11}^E, s_{33}^E, s_{33}^D can be determined.

The dielectric constants are determined by measuring capacitances of [100] and [001] orientated parallel plates. The capacitance were measured at 1 kHz using a Stanford Research System SR715 LCR meter. From the capacitance measurements, dielectric permittivities ϵ_{11}^T and ϵ_{33}^T were determined.

III. RESULTS AND DISCUSSION

The measured sound velocities for the eight pure modes are listed in Table I. Since none of these eight pure modes involves the elastic constants c_{13}^E or c_{33}^E, these two elastic constants must be derived from other quantities. Usually, the c_{33}^E is derived from the electromechanical coupling coefficient k_t and the elastic constant c_{33}^D by

$$c_{33}^E = c_{33}^D(1-k_t^2), \tag{1}$$

and c_{13}^E is calculated by

$$c_{13}^E = -\frac{s_{13}^E}{s}, \tag{2}$$

where

$$s_{13}^E = -\left[s_{33}^E \left(\frac{s_{11}^E c_{12}^E + s_{12}^E c_{11}^E}{c_{11}^E + c_{12}^E} \right) \right]^{1/2},$$
$$s = s_{33}^E(s_{11}^E + s_{12}^E) - 2(s_{13}^E)^2, \quad s_{12}^E = s_{11}^E - \frac{1}{c_{11}^E - c_{12}^E}. \tag{3}$$

Since it is much harder to make a resonator with the appropriate aspect ratio to measure the shear coupling coefficient k_{15}, its value is usually calculated by

$$k_{15}^2 = 1 - \frac{c_{44}^E}{c_{44}^D}. \tag{4}$$

TABLE II. Measured and derived material properties of PMN–33%PT multidomain single crystal poled in [001] (Density: $\rho=8060\ \mathrm{kg/m^3}$).

Elastic stiffness constants: c_{ij} ($10^{10}\ \mathrm{N/m^2}$)											
c_{11}^{E} [a]	c_{12}^{E}	c_{13}^{E}	c_{33}^{E}	c_{44}^{E} [a]	c_{66}^{E} [a]	c_{11}^{D}	c_{12}^{D}	c_{13}^{D}	c_{33}^{D} [a]	c_{44}^{D} [a]	c_{66}^{D}
11.5 ±0.15	10.3 ±0.16	10.2 ±0.15	10.3 ±0.3	6.9 ±0.05	6.6 ±0.05	11.7 ±0.15	10.5 ±0.15	9.0 ±0.35	17.4 ±0.5	7.7 ±0.05	6.6 ±0.05
Elastic compliance constants: s_{ij} ($10^{-12}\ \mathrm{m^2/N}$)											
s_{11}^{E} [a]	s_{12}^{E}	s_{13}^{E}	s_{33}^{E}	s_{44}^{E}	s_{66}^{E}	s_{11}^{D}	s_{12}^{D}	s_{13}^{D}	s_{33}^{D} [a]	s_{44}^{D}	s_{66}^{D}
69.0 ±2.0	−11.1 ±1.2	−55.7 ±1.2	119.6 ±4.0	14.5 ±0.1	15.2 ±0.2	44 ±1.0	−34 ±1.0	−4.1 ±1.0	11.1 ±0.8	13.0 ±0.1	15.2 ±0.18
Piezoelectric constants: e ($\mathrm{C/m^2}$)			d (10^{-12} C/N)			g (10^{-3} V m/N)			h (10^{8} V/m)		
e_{15}	e_{31}	e_{33}	d_{15}	d_{31} [a]	d_{33} [a]	g_{15}	g_{31}	g_{33}	h_{15}	h_{31}	h_{33}
10.1 ±0.9	−3.9 ±1.6	20.3 ±1.6	146 ±16	−1330 ±19	2820 ±75	10.3 ±0.6	−18.4 ±0.4	38.8 ±0.8	7.9 ±0.4	−5.9 ±2.0	33.7 ±1.7

Dielectric constants: ϵ (ϵ_0)				β ($10^{-4}/\epsilon_0$)				Electromechanical coupling constants				
ϵ_{11}^{S}	ϵ_{33}^{S}	ϵ_{11}^{T} [a]	ϵ_{33}^{T} [a]	β_{11}^{S}	β_{33}^{S}	β_{11}^{T}	β_{33}^{T}	k_{15}	k_{31} [a]	k_{33} [a]	k_{1} [a]	k_{p}
1434 ±110	680 ±45	1600 ±120	8200 ±200	7.0 ±0.1	14.7 ±0.5	6.30 ±0.1	1.2 ±0.1	0.32 ±0.02	0.59 ±0.01	0.94 ±0.01	0.64 ±0.01	0.77 ±0.04

[a]Measure properties.

Then, the piezoelectric strain constant d_{15} is determined by

$$d_{15}=k_{15}\sqrt{\epsilon_{11}^{T}s_{44}^{E}}. \tag{5}$$

After all the elastic stiffness constants c_{ij}^{E}, piezoelectric strain constant d_{ij}, and free dielectric permittivity ϵ_{ij}^{T} are obtained, other constants can be derived from constitutive equations. Finally, the whole set of elastic, piezoelectric, and dielectric constants of PMN–33%PT single crystal are obtained. The complete set of these material constants are shown in Table II. The errors were obtained from the average of properties measured using three batches of crystals with the same chemical composition. It is seen that the measured PMN–33%PT single crystal has larger d_{33} and k_{33} compared to PZN–4.5%PT.[8]

Based on the measured constants, the orientation dependence of sound velocity has been calculated by finding the eigenvalues and eigenvectors of Christoffel's tensor for given wave propagation directions. The calculated results for sound wave propagating in: (a) $X-Y$, (b) $Y-Z$ and (c) [110]-Z planes are shown Figs. 1(a)–1(c), where the length of a vector from the origin to any points on the curves gives sound velocity in that propagation direction. It is seen from Fig. 1 that the velocities of the longitudinal waves do not change as much as shear waves do for different propagation directions. The shear wave propagating in the $X-Y$ plane with its particle displacement also in the same plane, has the strongest orientation dependence as shown in Fig. 1(a). This shear wave velocity v_{s1} has a maximum (2882 m/s) in [100] and a minimum (about 880 m/s) in [110], respectively, which implies that a "soft shear acoustic mode" also exists in this domain-engineered single crystal system, similar to the PZN–4.5%PT case reported earlier.[8] Figure 1(b) shows that the phase velocity of the shear wave propagating and polarizing in the $Y-Z$ plane also changes drastically with the propagation direction. It has a maximum in [010] and a minimum in [011].

In order to further investigate the anisotropy of the multidomain PMN–PT single crystal system, some constant ratios are calculated. The calculated results are listed in Table III. Since there are no data available for the single domain single crystal PMN–PT system at the moment, the corresponding ratios for single crystal $BaTiO_3$ are listed in Table III for comparison. It is seen that the measured anisotropy of PMN–33%PT single crystal is comparable to the PZN–4.5%PT single crystal reported in Ref. 8 and it is generally less than that of single domain $BaTiO_3$. In particular, the dielectric anisotropy of measured PMN–33%PT is much smaller than that of $BaTiO_3$. This may be caused by the averaging effect of the multidomain structure of PMN–PT single crystals. On the other hand, the anisotropy for shear waves that propagate in the $X-Y$ plane with the displacement also in the same plane is larger for PMN–PT than for $BaTiO_3$. The "soft shear wave mode" along [110] is related to domain wall motion, since the dynamics of domain wall motions will contribute to the effective elastic compliance. The phase velocity of the shear wave that propagates along [110] and polarizes in [$1\bar{1}0$] is related to elastic compliance by

$$\nu=1/\sqrt{2\rho(s_{11}^{E}-s_{12}^{E})}. \tag{6}$$

Experimental results imply that the domain wall motion results in a very large effective $(s_{11}^{E}-s_{12}^{E})$, therefore, a slower sound velocity.

In order to obtain a complete set of self-consistent material properties from the measured data, proper analysis of measurement errors is very important. There are four equivalent kinds of piezoelectric constitutive equations for a piezoelectric system, which provide us with several control checks to minimize errors in those derived quantities. For each expression of derived quantities, errors will be introduced so that the same constant may be assigned different values

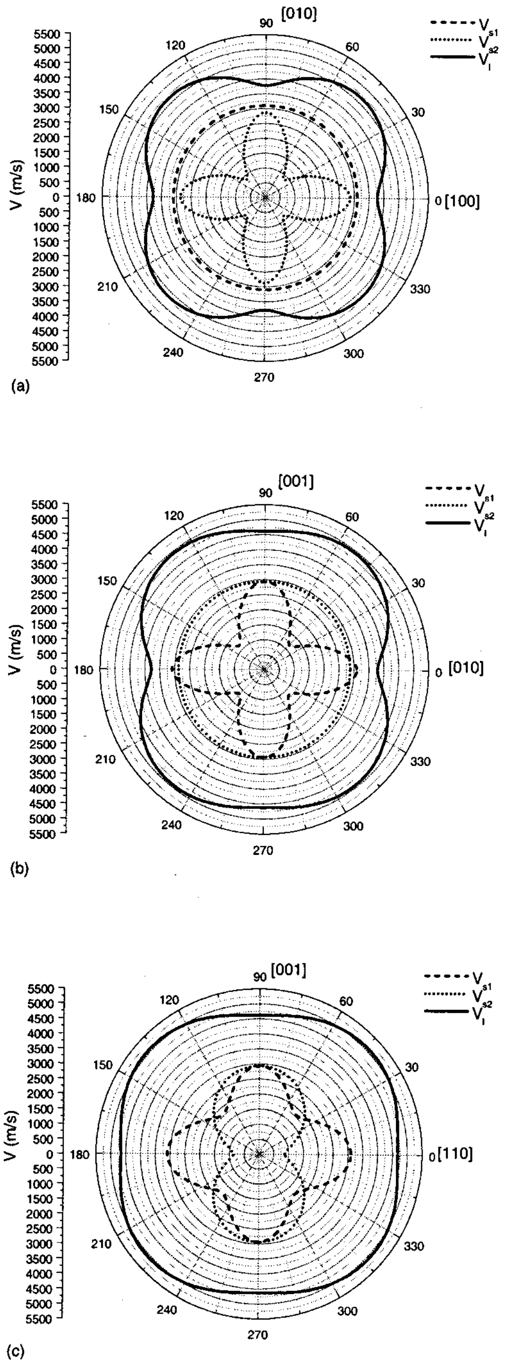

FIG. 1. Orientation dependence of the longitudinal velocity v_l and the shear velocities, v_{s1} and v_{s2}, respectively: (a) $X-Y$ plane, (b) $Y-Z$ plane, and (c) [110]-Z plane.

based on different formulas. For example, the c_{33}^E may be determined by Eq. (1), or by the following relation:

$$c_{33}^E = \frac{s_{11}^E + s_{12}^E}{s}. \tag{7}$$

When the measurement errors are large, the result obtained using Eq. (1) could be much different from the one obtained using Eq. (7). In sound velocity measurements, the resolutions of time of flight and sample thickness are 1 ns and 0.01 mm, respectively. For samples with 4 mm thickness, the relative error is about 0.1%. But nonperfect parallelness and misorientation limit the accuracy of sound velocity measurements to about 1%. The calculated orientation dependence of sound velocities can be used to estimate errors from misorientation. We found that the misorientation errors are very small for the longitudinal waves when the crystal orientations are done by the Laue method (within ±0.5°). But the orientation error can be serious for shear waves, especially for the shear wave propagating along the [110] with displacement in [$\bar{1}$10]. We also found that the value of the derived e_{31} is very sensitive to the uncertainty of c_{12}^E. A variation of 0.1% in c_{12}^E will cause substantial change in the value of e_{31}, sometimes, even change its sign. On the other hand, as analyzed above, it is very difficult to determine c_{12}^E, a derived quantity, with error less than 0.1% due to the limitation of the ultrasonic method. For this reason, resonance measurement is made using an edge excited thickness-vibration resonator. The thickness direction of the resonator is along [001] and the applied electric field is in the [100] direction. From the measured resonance and antiresonance frequencies, e_{31} can be derived with much higher accuracy. The result can be used to check the value of c_{12}^E and also to ensure the self-consistency of data listed in Table II.

In the measurements it is observed that the values of some elastic constants such as c_{33}^D are strongly dependent on the poling process. If the sample is not properly poled, the values of some elastic constants can change substantially since the constant D elastic constant values include large contribution from the piezoelectric effect. In order to check the poling status, d_{33} was also measured independently by the quasistatic method. Partial polarization reversal will cause the domain pattern to change and hence influence the macroscopic effective properties of the domain engineered single crystals. Therefore, ensuring a full polarization in the system is very important to obtain good electromechanical properties in the PMN–PT system.

TABLE III. Anisotropy of measured material properties of PMN–33%PT multidomain single crystal poled in [001].

Compound	$\epsilon_{11}^T/\epsilon_{33}^T$	$\epsilon_{11}^S/\epsilon_{33}^S$	s_{33}^E/s_{11}^E	s_{33}^D/s_{11}^D	s_{44}^E/s_{66}^E	s_{44}^D/s_{66}^E	s_{13}^E/s_{12}^E	s_{13}^D/s_{12}^D
PMN–PT	0.195	2.1	1.73	0.25	0.95	0.86	5.01	0.12
PZN–PT	0.596	3	1.32	0.33	0.98	0.94	1.79	0.18
$BaTiO_3$[a]	17.4	18.1	1.95	1.49	2.08	1.40	2.32	1.03

[a]See Ref. 12.

IV. SUMMARY AND CONCLUSIONS

0.67PMN–0.33PT single crystals poled along the [001] direction of the cubic axes were characterized by using both ultrasonic and resonance methods. A complete set of elastic, piezoelectric, and dielectric constants for the domain engineered single crystal PMN–33%PT system have been obtained. It was confirmed that the PMN–33%PT system has very large d_{33} and k_{33} coefficients. Based on the measured data, orientation dependence of the phase velocities of ultrasonic waves propagating in the $X-Y$, $Y-Z$, and [110]-Z planes has been calculated, and the anisotropy of material properties has been analyzed. We found that the anisotropy of phase velocities is very strong for shear waves, whereas it is relatively weak for the longitudinal waves. Similar to the case of PZN–4.5%PT reported in Ref. 8, a very slow shear wave with velocity of 880 m/s was found in the [110] direction with the displacement in [$\bar{1}$10]. The soft shear wave mode is associated with domain wall motions. This complete set of material property data not only will provide the necessary input for device design using these crystals, it will also provide bases for further theoretical studies on the principles of the domain engineering process.

ACKNOWLEDGMENTS

This research was sponsored by the ONR/DARPA under Grant No. N00014-98-1-0527. Crystals used for this study were provided by Dr. T. R. Shrout, Dr. P. Rehrig, and Dr. S. Zhang through the Piezocrystal Resource Center of the Pennsylvania State University. The authors would also like to thank Professor Wenhua Jiang for helpful discussions on the characterization techniques.

[1] S. E. Park and T. R. Shrout, J. Appl. Phys. **82**, 1804 (1997).
[2] H. Luo, G. Xu, P. Wang, and Z. Yin, Ferroelectrics **231**, 97 (1999).
[3] Z. Yin, H. Luo, P. Wang, and G. Xu, Ferroelectrics **229**, 207 (1999).
[4] M. Dong and Z. G. Ye, J. Cryst. Growth **209**, 81 (2000).
[5] S. Nomura and Uchino, Ferroelectrics **50**, 107 (1983).
[6] S. Park, P. Lopath, K. Shung, and T. Shrout, Proc. SPIE **3037**, 140 (1997).
[7] S. E. Park and T. R. Shrout, IEEE Trans. Ultrason. Ferroelectr. Freq. Control **44**, 1140 (1997).
[8] J. Yin, B. Jiang, and W. Cao, IEEE Trans. Ultrason. Ferroelectr. Freq. Control **47**, 285 (2000).
[9] ANSI/IEEE STD. 176-1987, *IEEE Standard on Piezoelectricity* (IEEE, New York, 1987).
[10] A. W. Warner, M. Onoe, and G. A. Coquin, J. Acoust. Soc. Am. **42**, 1223 (1967).
[11] S. Zhu, B. Jiang, and W. Cao, Proc. SPIE **3341**, 154 (1998).
[12] D. A Berlincourt, D. R. Curran, and H. Jaffe, in *Physical Acoustics*, edited by W. P. Mason, Vol. 1A, p. 218.